 doi:10.20944/preprints202012.0749.v1

SARS-CoV-2 Nsp5 Protein Causes Acute Lung Inflammation: A Mathematical Model

Antonio Bensussen[1], Elena R. Álvarez-Buylla[2,*], José Díaz[1,*]

[1]Laboratorio de Dinámica de Redes Genéticas, Centro de Investigación en Dinámica Celular, Universidad Autónoma del Estado de Morelos, Cuernavaca, Morelos, México.

[2] Centro de Ciencias de la Complejidad (C3), Universidad Nacional Autónoma de México, Ciudad de México, México.

*** Correspondence:**

José Díaz
biofisica@yahoo.com; jose.diaz@uaem.mx

Elena R. Álvarez Buylla
eabuylla@protonmail.com

Keywords: SARS-CoV-2 infection, Interleukin 6; NFκB; Nsp5; Cox2; SARS-CoV-2 interactome; Nonlinear dynamics of inflammation

Abstract

In the present work we propose a mathematical model of the process of inflammation in lung cells in response to SARS-CoV-2 infection from which a plausible scenario for the dynamics of this process arise. In this scenario the main protease Nsp5 enhances the inflammatory process, increasing the levels of NF κB, IL-6, Cox2, and PGE2 with respect to a reference state without the virus. When in presence of the virus the translation rates of NF κB and IκB are increased to a high constant value, and the translation rate of IL-6 is increased above the threshold value of 7 nM s^{-1}, the model predicts a persistent over stimulated immune state with high levels of the cytokine IL-6. This over stimulated immune state becomes autonomous of the signals from other immune cells like macrophages and lymphocytes, and does not shut down by itself. Dexamethasone or Nimesulide have little effect on this state of the infected lung cell, and the only form to suppress it is with the inhibition of the activity of the viral protein Nsp5 with drugs like Saquinavir. In this form, our model suggests that Nsp5 is effectively the cause of the severe acute lung inflammation during SARS-CoV-2 infection. The persistent production of IL-6 by lung cells can be one of the causes of the cytokine storm observed in critical patients with COVID19. From an evolutive point of view, the use of Nsp5 as the switch to start inflammation, and the consequent overproduction of the ACE2 receptor, is the probable reason of the increased dangerousness of SARS-CoV-2 with respect to SARS-CoV.

Preprints (www.preprints.org) | NOT PEER-REVIEWED | Posted: 30 December 2020 doi:10.20944/preprints202012.0749.v1

1 Introduction

Severe Acute Respiratory Syndrome Coronavirus 2 (SARS-CoV-2) virus is an intracellular parasite whose replication cycle depends on host cell structures and functions. In particular, it uses the translational apparatus of different types of infected cells to express its proteins (Nakagawa et al., 2016). SARS-CoV-2 causes the Coronavirus Disease 2019 (COVID19), which has infected around ~ 65,000,000 persons worldwide since the end of 2019 and killed about ~ 1,500,000 of them. There are not therapeutic drugs to defeat SARS-CoV-2 infection in this moment (Díaz, 2020a), although a vaccine with 95% of effectiveness will be soon available.

SARS-CoV-2 virion is formed by four proteins: spike (S), envelope (E), membrane (M) and nucleocapside (N) that enclose the virus genome (McBride and Fielding, 2012), which consists of a positive-sense nonsegmented single stranded mRNA ((+)ssRNA) of 30 kb. The open reading frames 1a (orf1a) and 1b (orf1b) are located near the untranslationd region 5' (5'UTR) of the positive single stranded RNA ((+)ssRNA) and they code for the polyproteins pp1a and pp1ab.

When SARS-CoV-2 virion infects the organism, S protein binds with high affinity to the surface receptor Angiotensin-Converting Enzyme 2 (ACE2), highly abundant in the lung alveolar type II cells and other cell types (Gordon et al., 2020; Hamming et al, 2004), and forms a molecular complex that begins the process of fusion of the virion envelope with the host cell membrane. Finally, viral (+)ssRNA is released into the host cytoplasm (Letko et al., 2020) (Figure 1).

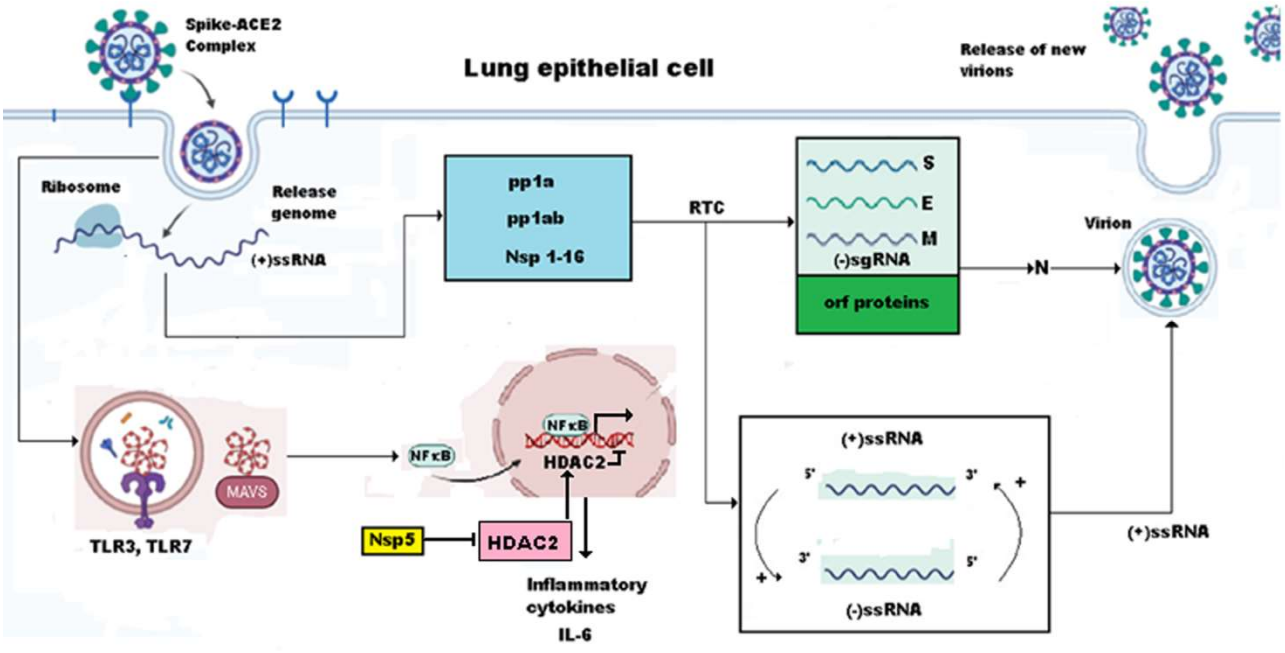

Figure 1.- Process of infection of lung cells by SARS-CoV-2. Infection begins when the protein S of the virion binds with high affinity to the cells surface receptor ACE2 (Angiotensin-Converting Enzyme 2) that is highly abundant in the lung alveolar type II cells. The formation of the complex S-ACE2 initiates the process of fusion between the virion envelope and the cells membrane leading to the liberation of the nucleocapside with the viral genome into the cytoplasm .SARS-CoV-2 genome consists of a positive-sense nonsegmented single stranded mRNA ((+)ssRNA) of ~ 30 kb. The open reading frames 1a (orf1a) and 1b (orf1b) are located near the 5'UTR of the (+)ssRNA and they code for the polyproteins pp1a and pp1ab. Maturation of these polyproteins results in 11 nonstructural proteins (Nsp) from the orf1a segment (Nsp1 to Nsp11) and 5 nonstructural proteins from the orf1b segment (Nsp12 to Nsp16). Nsp proteins form the replication-

Preprints (www.preprints.org) | NOT PEER-REVIEWED | Posted: 30 December 2020 doi:10.20944/preprints202012.0749.v1

transcription complex (RTC) a set of nested subgenomic minus-strands of RNA ((-)sgRNA) are synthesized in a process of discontinuous transcription. These (-) sgRNAs serve as the templates for the production of subgenomic mRNAs from which the structural proteins E, M, N and S, together with the accessory proteins orf 3a, orf6, orf7a, orf7b, orf8, orf9b, orf9c and orf10 are synthesized. The presence of viral (+)ssRNA initiates the TLR3 and TLR4 mediated immune response, which increases the concentration of free NF κB in cytoplasm. Cytoplasmic NF κB enters the nucleus where promotes the transcription of a series of target genes. Viral protein Nsp5 inhibits the inhibition exerted by HDAC2 on nuclear NF κB transcription factor, enhancing the synthesis of inflammatory cytokines like IL-6. (Figure drawn using Biorender template https://app.biorender.com/).

The process of translation occurs in the cytoplasm and produces a set of viral polyproteins whose maturation results in 11 nonstructural proteins (Nsp) from the orf1a segment (Nsp1 to Nsp11) and 5 nonstructural proteins from the orf1b segment (Nsp12 to Nsp16). Nsp proteins form the replication-transcription complex (RTC) in a double-membrane vesicle where a set of nested subgenomic minus-strands of RNA ((-)sgRNA) are synthesized in a process of discontinuous transcription. These (-) sgRNAs serve as the templates for the production of subgenomic mRNAs from which the structural proteins E, M, N and S, together with the accessory proteins orf 3a, orf6, orf7a, orf7b, orf8, orf9b, orf9c and orf10 are synthesized (Díaz, 2020a; Sevajol et al., 2014; Dongwan et al., 2020). SARS-CoV-2 uses the host translational machinery to redirect it to viral protein synthesis and replication, while host mRNA translation is inhibited (Nakagawa et al., 2016). SARS-CoV and SARS-CoV-2 genomes have ~ 79% of homology (Forster et al., 2020), and most of the set of structural and nonstructural proteins are practically the same. However, the virus species differ in the accessory proteins orf8, orf8a, orf 8b, orf9c and orf10 (Bartlam et al., 2005; Gordon et al., 2020) (Table 1).

Table 1.- Equations and parameters of the basic model of inflammation

Basic Inflammation Circuit	**Parameters**
$\frac{dNF\kappa B}{dt} = V_{nf}^{\max} p_{nf}^{on}(t) + k_1 \cdot il6 \cdot i\kappa bnf + k_{11} pge2 \cdot i\kappa bnf - k_4 i\kappa b \cdot nf - D \cdot nf$ $i\kappa bn = I\kappa B - NF\kappa B$ molecular complex	$k_1 = 0.5$ nM^{-1}s^{-1} $k_4 = 5$ nM^{-1}s^{-1} $D = 1$ s^{-1}
$\frac{d(nf^*)}{dt} = D\left(\frac{V_{cyt}}{V_{nuc}}\right) nf - k_{\deg} nf^*$ nf^* = nuclear concentration of $NF\kappa B$	$k_{deg} = 2$ s^{-1} $\left(\frac{Vcyt}{Vnuc}\right) = 2$
$\frac{d(i\kappa bnf)}{dt} = k_4 nf \cdot i\kappa b - k_5 il6 \cdot i\kappa bnf - k_{11} pge2 \cdot i\kappa bnf$ $i\kappa bnf = I\kappa B - NF\kappa B$ molecular complex $pge2$ = amount of PGE2	$k_4 = 5$ nM^{-1}s^{-1} $k_5 = 0.5$ nM^{-1}s^{-1}
$\frac{dp_{IL6}^{on}(t)}{dt} = k_2 \frac{nf^*}{hd^*+1} p_{IL6}^{off}(t) - k_{-2} p_{IL6}^{on}(t)$ $p_{IL6}^{on}(t)$ = probability of $IL6$ activation at time t hd^* = amount of HDAC2 in nucleus	$k_2 = 0.1$ (Number of Molecules)$^{-1}$s^{-1} $k_{-2} = 0.035$ s^{-1}

Preprints (www.preprints.org) | NOT PEER-REVIEWED | Posted: 30 December 2020 doi:10.20944/preprints202012.0749.v1

$\frac{dp^{on}_{I\kappa B}(t)}{dt} = k_3 \frac{nf^*}{hd^*+1}\left(1 - p^{on}_{I\kappa B}(t)\right) - k_{-3} p^{on}_{I\kappa B}(t)$ $p^{on}_{I\kappa B}(t)$ = probability of $I\kappa B$ activation at time t	k_3 = 0.1 (Number of Molecules)$^{-1}$s^{-1} $k_{\_3}$ = 0.035 s^{-1}
$\frac{dp^{on}_{Cox2}(t)}{dt} = k_7 \frac{nf^*}{hd^*+1}\left(1 - p^{on}_{Cox2}(t)\right) - k_{-7} p^{on}_{Cox2}(t)$ $p^{on}_{Cox2}(t)$ = probability of $Cox2$ activation at time t	k_7 = 0.1 (Number of Molecules)$^{-1}$s^{-1} $k_{\_7}$ = 0.035 s^{-1}
$\frac{dp^{on}_{NF\kappa B}(t)}{dt} = k_{15} \frac{nf^*}{hd^*+1}\left(1 - p^{on}_{NF\kappa B}(t)\right) - k_{-15} p^{on}_{NF\kappa B}(t)$ $p^{on}_{NF\kappa B}(t)$ = probability of $NF\kappa B$ activation at time t	k_{15} = 0.1 (Num of Molecules)$^{-1}$s^{-1} $k_{\_15}$ = 0.035 s^{-1}
$\frac{d(nsp5)}{dt} = \phi - k_{18} nsp5$ $nsp5$ = amount of viral Nsp5 in cell ϕ = rate of Nsp5 production	k_{18} = 0.7 s^{-1} ϕ = 14 nM s^{-1}
$\frac{d(hd)}{dt} = \frac{r}{nsp5+1} - D_2 \cdot hd$ hd = amount of HDAC2 in cytoplasm D_2 = transport constant of HDAC2	r = 30 nM s^{-1} D_2 = 2 s^{-1} η = 1 nM^{-1}
$\frac{d(hd^*)}{dt} = D_2\left(\frac{V_{cyt}}{V_n}\right) hd - k_{\deg 2} hd^*$	D_2 = 2 s^{-1} k_{deg2} = 2 s^{-1} $\left(\frac{Vcyt}{Vnuc}\right) = 2$
$\frac{d(il6)}{dt} = \alpha(t) + V^{\max}_{IL6} p^{on}_{IL6}(t) - k_5 \cdot il6 \cdot i\kappa bnf - k_6 il6$	k_5 = 0.5 nM^{-1}s^{-1} k_6 = 0.5 s^{-1} $\alpha(t)$ = 10 nM s^{-1}
$\frac{d(i\kappa b)}{dt} = V^{\max}_{I\kappa B} p^{on}_{I\kappa B}(t) - k_4 i\kappa b \cdot nf$	k_4 = 5 nM^{-1}s^{-1}
$\frac{d(cox2)}{dt} = V^{\max}_{Cox2} p^{on}_{Cox2}(t) - k_{10} cox2$	k_{10} = 0.4
$\frac{d(pge2)}{dt} = k_{17} cox2 - k_{11} pge2 \cdot i\kappa bnf - k_{12} pge2$	k_{17} = 0.8 s^{-1} k_{11}= 0.8 nM$^{-1}s^{-1}$ k_{12} = 3 s^{-1}

In the reference state the translation velocities are: $V^{\max}_{nf} = V^{\max}_{Cox2} = V^{\max}_{IL6} = V^{\max}_{I\kappa B} = 2$ nM s^{-1}

Viral proteins are inserted into the host molecular machinery to modify and redirect a great number of host cell functions towards the production of more virus particles (Masters, 2006; Wu et al., 2020). Experimental analysis of the interaction of viral and host proteins, or *interactome*, by Gordon and collaborators (Gordon et al., 2020) has been a fundamental contribution to understand the form in which SARS-CoV-2 virus takes control of the host molecular network to produce new

Preprints (www.preprints.org) | NOT PEER-REVIEWED | Posted: 30 December 2020 doi:10.20944/preprints202012.0749.v1

virions and propagate the infection. Gordon and collaborators (2020) cloned, tagged and expressed 26 viral proteins in human cells using affinity- purification mass spectrometry to identify the human proteins physically associated with each other. They found around 332 SARS-CoV-2-human protein-protein interactions that constitute the virus interactome. From these results, the construction of the network representation of the interactome is possible.

Formulation of network models is a tool to understand the organization and dynamics of complex systems (Breitling, 2010). A theoretical approach to biological networks structure and function allows the integration of disperse experimental data in a coherent model of the spatio-temporal dynamics of interconnected cellular processes (Díaz, 2020a). The number of nodes, the number of connections of each node to his neighbours, and the distribution of these connections in the network determine its complexity, structure and dynamical properties (Kumar et al., 2015). In the particular case of the Gordon interactome, the analysis of its undirected network model indicates a modular free-scale hierarchical type of structure in which proteins orf8, N and Nsp7 are the main hubs (Díaz, 2020a).

In this network, the viral main protease Nsp5 has a special role in lung inflammation through its link with Histone Deacetylase 2 (HDAC2) (Díaz, 2020a; Gordon et al., 2020) (Figures 1 and 2); suggesting that Nsp5 role is to inhibit HDAC2 inhibitory action on NF κB (Figure 1), and enhance the transcription of the pro-inflammatory genes targeted by the Nuclear Factor κB (NF κB) (Figures 1 and 2) (Wagner et al., 2015), which is the difference between SARS-CoV and SARS-CoV-2. The virus SARS-CoV uses N protein to promote the sustained transcription of the Cyclooxygenase 2 (Cox2) enzyme by binding directly to the NF-κB transcriptional regulatory elements and to CCAAT/enhancer binding proteins of the gene *Cox2* (Yan et al., 2006). In consequence, SARS-CoV and SARS-CoV-2 produce the severe acute respiratory syndrome through different mechanisms.

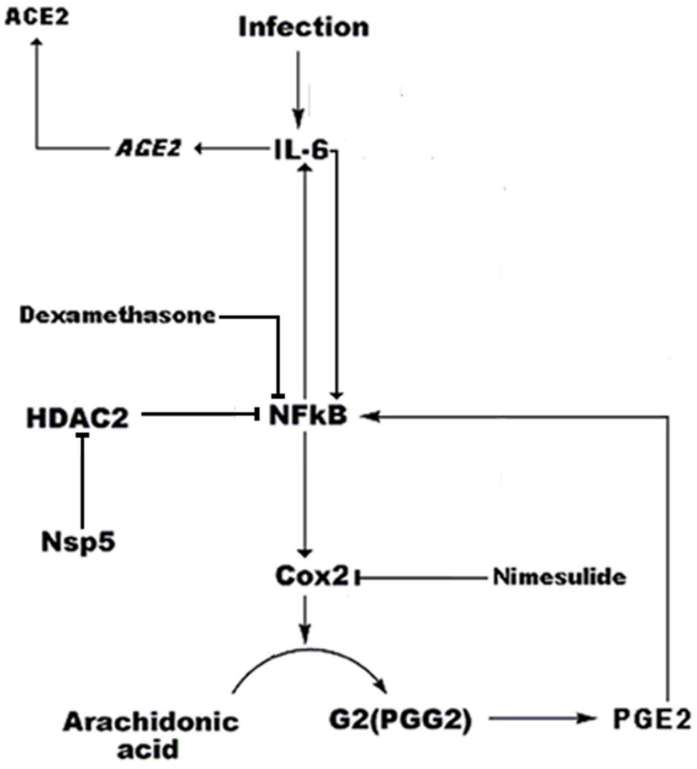

Preprints (www.preprints.org) | NOT PEER-REVIEWED | Posted: 30 December 2020 doi:10.20944/preprints202012.0749.v1

Figure 2.- Circuit representation of inflammation. IL-6, NF κB, Cox2, and PGE2 are the basic nodes of the circuit that represents the basic features of inflammation of lung cells during SARS-CoV-2 infection. In this circuit the arrows represent activation and the bars inhibition. In the figure are shown two positive feedback loops between IL-6 and NF κB, and between NF κB and Cox2. IL-6 also induces the expression of the ACE2 receptor in the lung cell membrane. NF κB is inhibited by HDAC2, which in turn is inhibited by the viral protein Nsp5. The circuit has two targets for the anti-inflammatory drugs Nimesulide and Dexamethasone.

The change from a hub (N protein in SARS-CoV) to a single poor connected protein (Nsp5 in SARS-CoV-2) as the cause of severe acute respiratory syndrome could be an evolutive adaptation that increases SARS-CoV-2 pathogenicity. Malfunction or deletion of Nsp5 does not necessarily stop the viral replication cycle (Cohen et al., 2000) (Figure 1). Thus, Nsp5 is a molecular switch whose deletion or malfunctioning only decreases the strength of inflammation and the persistence of ACE2 in the lung epithelial cells giving rise to a less intense inflammatory response (Long et al., 2020).

Activation of the NF κB family of proteins (p65/RelA, p105/p50, p100/p52, RelB, and c-Rel) consist in the phosphorylation of the inhibitor of NF κB proteins (IκBs) by IκB kinases (IKKs) and the posterior ubiquitinylation and degradation of the phosphorylated IκBs (Figure 1). The released NF κB proteins enter the nucleus to activate specific genes (Wagner et al., 2015). In the nucleus, HDAC2 blocks the transcriptional activity of NF κB, inhibiting the production and release of the cytokine Interleukin 6 (IL-6) and IκB, and interfering with the functioning of the positive feedback circuit between IL-6 and NF κB (Rahman, and MacNee, 1998) (Figure 3a). As we mentioned before, the sustained inactivation of HDAC2 by Nsp5 produces a sustained increase in the transcriptional activity of NF κB (Figures1 and 2) that leads to a high production of IL-6 in the lung epithelium cells. Release of this excess of IL-6 to the vascular system contributes to the "cytokines storm" observed in critical patients (Magro, 2020). The uninterrupted production of IL-6 generates a persistent presence of the ACE2 receptor in the lung cells membranes due to enhanced *ACE2* expression mediated by the JAK-STAT pathway (Hennighausen and Lee, 2020) (Figure 2).

NF κB also promotes *Cox2* transcription leading to the expression and increased enzymatic activity of Cox2 (Figures 2 and 3B). However, NF κB, Cox2 and IL-6 also form a positive feedback circuit in which NF κB promotes Cox2 enzymatic activity that catalyses the conversion of Arachidonic acid (AA) into Prostaglandin G2 (PGG2), which is in turn modified by the peroxidase moiety of the Cox2 enzyme to produce prostaglandin H2 (PGH2) that is converted to prostaglandin E2 (PGE2) (Alexanian and Sorokin, 2017). PGE2 is then released to the vascular system, binds to its membrane EP2 and EP4 prostanoid receptors and promotes the cleavage of the IκB-NF κB complex increasing the amount of free NF κB, which increases the production of IL-6 (Figure 3B) (Cho et al., 2014; Bouffi et al., 2010). IL-6, in turn, increases NF κB activity (Wang et al., 2003) (Figure 2). These regulatory circuits has three therapeutic targets: IL-6 production (Tocilizumab) (Magro 2020), Cox2 (Nimesulide) (Alexanian and Sorokin, 2017) and NF κB (Dexamethasone) (Newton et al., 1998; Aghai et al, 2006).

In this work, we propose that the three feedback loops mentioned above constitute the minimal circuit for the inflammatory process of epithelial lung cells during SARS-CoV-2 infection (Figure 2), and we use an ordinary differential equations (ODEs) continuous model to explore the effect of Nsp5 in the qualitative dynamics of this circuit in which this viral protein acts as an enhancing perturbation in the phase space of this dynamical system (Diaz, 2020b) (Figure 2). For the modeling

Preprints (www.preprints.org) | NOT PEER-REVIEWED | Posted: 30 December 2020 doi:10.20944/preprints202012.0749.v1

of the circuit, we chose as main nodes NF κB, IκB, IL-6, Cox2, and PGE2. In the model, Nsp5 prevents the movement of HDAC2 into the nucleus allowing an increase in NF κB transcriptional activity. The input that turns *on* the circuit in lung cells is a signal from monocytes, lymphocytes, and other immune cells that activates IL-6 production. We propose that this model represents the basic main interactions that settles *on* the inflammation reaction to the invasion of the lung cells by SARS-CoV-2, and that is a first approximation to understand the main dynamical features of this response.

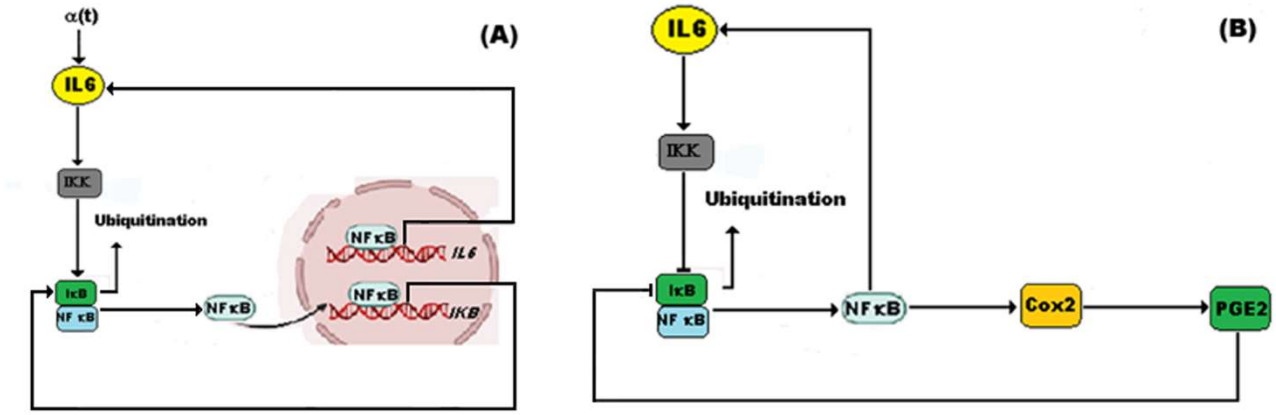

Figure 3.- Feedback loops of the model of inflammation. The mathematical model proposed in this work is based on the dynamical features of three feedback loops: A) two positive feedback loops between IL-6 and NF κB, and NF κB and IκB; B) a negative feedback loop between PGE2 and IκB. In Figure A, $\alpha(t)$ is a external signal that represents the amount of IL-6 produced by immune cells like monocytes and lymphocytes, among others.

SARS-CoV-2 infection.

Our hypothesis is that Nsp5 leads to the sustained overproduction of IL-6, Cox2, PGE2, and NF κB, in the epithelial lung cells, which is *a necessary but not a sufficient condition* for a cytokine storm. In particular case of the epithelial lung cells. We found that the computational and mathematical analysis of the model supports our hypothesis, and that Nsp5 effectively enhances NF κB, IL-6, Cox2 and PGE2 production during the time that remains bounded to HDAC2. Furthermore, the model predicts the existence of an over stimulated immune state (OSIS) in which the amount of IL-6 produced by the infected lung cells is very high and independent of any stimulus from external sources like monocytes, and lymphocytes. The OSIS cannot be shut down by classical anti-inflammatory drugs like Nimesulide and Dexamethasone, and can be beaten only with specific inhibitors of Nsp5 like Saquinavir (Xu et al., 2020).

2 Model

Immune response to infections is a complex process in time and space in which numerous molecules and cells act with high specificity, different timing and different spatial distributions. In consequence, the immune response to infections is a multiscale process in which innate and acquired immunity protect the organism against pathogens (Eftimie et al, 2016). In this scenario, the number of necessary variables for a detail description of the spatio-temporal dynamics of the immune system is tremendously high (although some computational efforts have been made in this direction (Danos et al., 2007), and imposes severe obstacles for the statement of continuous

Preprints (www.preprints.org) | NOT PEER-REVIEWED | Posted: 30 December 2020 doi:10.20944/preprints202012.0749.v1

quantitative models. The lack of quantitative experimental data, and the ignorance of the value of most of the model parameters, increase the difficulty of a detailed quantitative modeling of the immune response to infections and leave a qualitative approach as an alternative (Eftimie et al., 2016).

In this framework, ordinary differential equations (ODEs) qualitative modeling is oriented to determine all the possible trajectories of a dynamical system (system that varies in time) along its *n*-dimensional phase space (with $n > 0$), when the system is subject to a set of initial conditions and parameters values. High dimensional nonlinear dynamical systems can exhibit a variety of coexisting dynamical behaviors that determine the structure of their phase space (Strogatz, 2015). However, the structure of the phase space of biological nonlinear dynamical systems is highly dependent on the set of parameters values. Variations in the value of one or more parameters can drive a drastic change in phase space generating a different qualitative dynamics of the system. This process is known as bifurcation and is of important to find the possible bifurcations in the system and to identify which parameter or parameters are the responsible of these changes (Strogatz, 2015)(See Supplementary Material 2 (SM 2)).

In order to avoid the problem due to the high dimensionality and complexity of the immune response to SARS-CoV-2 infection, and to use the minimum number of parameters in the model that we are proposing in this work, we assume that the interaction between nodes IL-6, NF κB, IκB, Cox2 and PGE2 settles on the main dynamical features of the inflammation process in lung epithelial cells due to the presence of the Nsp5 viral protein. In this circuit of Figure 2, IL-6, NF κB, Cox2 and PGE2 define three feedback loops (Figures 3A-3B): a positive feedback loop between NF κB and IL-6 (Figure 3A); a positive feedback loop between NF κB and IκB (Figure 3A); and a negative feedback loop between PGE2 and IκB (Figure 3B).

These feedback loops are distributed between three compartments:

a) IL-6 is secreted into the extracellular medium where acts in paracrine and exocrine form. IL-6 binds to its receptor IL6R at the cell surface. Once the complex IL6-IL6R is formed, it activates IKK in the cytoplasm (Wang et al, 2003). PGE2 is also secreted into this compartment where it binds to EP2 and EP4 receptors at the cell surface, activating Protein Kinase B (Akt) in the cytoplasm (Cho et al., 2014).

b) IKK, free NF κB, and the complex IκB-NF κB are located in the cytoplasm, where IκB is degraded by ubiquitination. Protein Cox2 is located in the endoplasmic reticulum (ER).

c) Free NF κB enters the nucleus where induce the transcription of *IL6*, *Cox2*, *IKB* and *NF κB* genes. Transcriptional activity of nuclear NF κB is inhibited by HDAC2, and enhanced by Nsp5.

In this form, the model cell consists of three compartments: extracellular medium, cytoplasm and nucleus. We assume that the ratio of the cytoplasmatic volume to external volume (V_{cyt} / V_{out}) is one, and that the radio of the cytoplasmatic volume to the nuclear volume (V_{cyt} / V_{nuc}) is 2. In each compartment the concentration of the molecules are measured in nanomolar (nM).

In the circuit of Figure 2, the rate of production of free cytoplasmic NF κB depends on the rate of its release from the IκB-NF κB complex, which is proportional to the product of the concentrations of IκB and IKK (Figure 3A), its own rate of production due to nuclear NF κB transcriptional

Preprints (www.preprints.org) | NOT PEER-REVIEWED | Posted: 30 December 2020 doi:10.20944/preprints202012.0749.v1

activity inhibited by HDAC2 (Figures 1 and 3A), the rate at which is recaptured by IκB (Figure 3A), and the rate of transport into the nucleus:

$$\frac{d(nf)}{dt} = V_{nf}^{\max} p_{nf}^{on}(t) + k_a ikk \cdot i\kappa bnf - k_4 nf \cdot i\kappa b - D \cdot nf \qquad (1)$$

where *nf* is the concentration of free NF κB, $V_{nf}^{\max}$ is the maximum rate of translation of the NF κB gene, $p_{nf}^{on}(t)$ is the probability that the NF κB gene is its active state (*on*), *ikk* is the concentration of IKK, *iκbnf* is the concentration of IκB-NF κB complex, k_a and k_2 are rate constants and *D* is the transport constant (Table 1) .

We assume that the concentration of IKK activated by IL-6 is proportional to the external concentration of the cytokine: $ikk = \gamma_1 \cdot il6$, where γ_1 is a constant of proportionality. In a similar form, PGE2 increases the rate of cleavage of the complex IκB-NF κB by phosphorylation of the IKKα subunit by Akt (Bai et al, 2009)(Figure 3B). Thus, we assume that the concentration of Akt is proportional to the external concentration of PGE2: $akt = \gamma_2 \cdot pge2$. Substituting both expressions in Eq. (1) we finally obtain:

$$\frac{d(nf)}{dt} = V_{\max nf} p_{nf}^{on}(t) + k_1 il6 \cdot i\kappa bnf + k_{11} pge2 \cdot i\kappa bnf - k_4 nf \cdot i\kappa b - D \cdot nf \qquad (2)$$

where k_1 and k_{11} are the new rate constants (Table 1).

The rate at which the complex IκB-NF κB is broken in presence of IKK depends on the rate at which IKK and Akt remove IκB from the complex under the action of IL-6 and PGE2, and the rate at which the complex is formed again.:

$$\frac{d(i\kappa bnf)}{dt} = k_4 nf \cdot i\kappa b - k_5 il6 \cdot i\kappa bnf - k_{11} pge2 \cdot i\kappa bnf \qquad (3)$$

where *iκbnf* is the concentration of the complex IκB-NF κB, and k_4 and k_5 are rate constants (Table 1).

The rate at which NF κB enter the nucleus depends on the rate of transport of the molecule into de nucleus, adjusted for the change in volume between the cytoplasmic and nuclear compartments, and on the rate of inhibition of nuclear NK κB by its inhibitors:

$$\frac{dnf^*}{dt} = D\left(\frac{V_{cyt}}{V_{nuc}}\right) nf - k_{\deg} nf^* \qquad (4)$$

where *nf** is the nuclear concentration of NF κB and k_{deg} is a rate constant.

The probabilities of activation of genes *IL6*, *Cox2*, *IκB* and *NF κB* (Figures 3A and 3B) are given by:

Preprints (www.preprints.org) | NOT PEER-REVIEWED | Posted: 30 December 2020 doi:10.20944/preprints202012.0749.v1

$$\frac{dp_{IL6}^{on}(t)}{dt} = k_2\left(\frac{nf^*}{hd^*+1}\right)\left(1-p_{IL6}^{on}(t)\right)-k_{-2}p_{IL6}^{on}(t) \qquad (5)$$

$$\frac{dp_{I\kappa B}^{on}(t)}{dt} = k_3\left(\frac{nf^*}{hd^*+1}\right)\left(1-p_{I\kappa B}^{on}(t)\right)-k_{-3}p_{I\kappa B}^{on}(t) \qquad (6)$$

$$\frac{dp_{Cox2}^{on}(t)}{dt} = k_7\left(\frac{nf^*}{hd^*+1}\right)\left(1-p_{Cox2}^{on}(t)\right)-k_{-7}p_{Cox2}^{on}(t) \qquad (7)$$

$$\frac{dp_{NF\kappa B}^{on}(t)}{dt} = k_{15}\left(\frac{nf^*}{hd^*+1}\right)\cdot\left(1-p_{NF\kappa B}^{on}(t)\right)-k_{-15}p_{NF\kappa B}^{on}(t) \qquad (8)$$

see Supplementary Material I (SM I) for the mathematical deduction of these equations. For Eqs. 5-7, $p_i^{on}(t)$, $i \in \{\text{IL-6, I}\kappa\text{B, Cox2, NF }\kappa\text{B}\}$, is the probability that the gene *i* is expressed at time *t*, *hd** is the amount of HDCA2 in nucleus, and k_2, k_{-2}, k_3, k_{-3}, k_7, k_{-7}, k_{15}, k_{-15} are rate constants (Table 1).

We assume that free cytoplasmic HDAC2 is produced according to the rate equation:

$$\frac{d(hd)}{dt} = \frac{r}{\eta(nsp5+1)} - D_2 \cdot hd \qquad (9)$$

where *hd* is the amount of free cytoplasmic HDAC2 that is produced at a constant rate *r*, D_2 is the rate of transport of free HDAC2 into the nucleus. In this equation, nsp5 is the amount of Nsp5 in the infected cell that sequester HDAC2 in cytoplasm (El Baba & Herbein, 2020), and η is a constant (Table 1). Free cytoplasmic HDCA2 enters the nucleus according to the equation:

$$\frac{d(hd^*)}{dt} = D_2\left(\frac{V_{cyt}}{V_n}\right)hd - k_{\deg 2}hd^* \qquad (10)$$

where k_{deg2} is a rate constant (Table 1).

Nsp5 is a protein with only one link to the virus interactome (Gordon et al., 2020; Díaz. 2020a), which is an input to the circuit of Figure 2. However, the real kinetic mechanism of action of this viral protein is unknown, thus we assume a plausible simple kinetic mechanism for its production in the system in which we set the parameters ϕ and k_{18} to the values shown in Table 1 that leads Nsp5 to have a maximum constant value of 20 nM:

$$\frac{d(nsp5)}{dt} = \phi - k_{18}nsp5 \qquad (11)$$

where ϕ is the constant rate of production of Nsp5, and k_{18} is a rate constant (Table 1).

During the early stage of infection by SARS-CoV-2, the rate of variation of the concentration of IL-6 outside the lung cell depends on the rate of production of IL-6 by monocytes, leucocytes and other

Preprints (www.preprints.org) | NOT PEER-REVIEWED | Posted: 30 December 2020 doi:10.20944/preprints202012.0749.v1

cells under stimulation by Tall-like Receptors (TLRs) (denoted by $\alpha(t)$) (Magro, 2020; Jafarzadeh et al, 2020), on the rate of production by lung cells due to nuclear NF κB transcriptional activity enhanced by Nsp5 (Figure 3A), and on the rate of degradation of IL-6 by different mechanisms. Finally, we assume that the concentration of IKK activated by IL-6 is proportional to the external concentration of the cytokine (see Eq. 2):

$$\frac{d(il6)}{dt} = \alpha(t) + V_{IL6}^{\max} p_{IL6}^{on}(t) - k_5 il6 \cdot i\kappa bnf - k_6 il6 \qquad (12)$$

where $V_{IL6}^{\max}$ is the maximum rate of translation of *IL6*, $p_{IL6}^{on}(t)$ is the probability that the gene *IL6* is activated at time *t*, k_5 and k_6 are rate constants (Table 1).

The rate of variation of the amount of free IκB in the system is the balance between the rate of translation of gene *IκB* and the rate of formation of new IκB-NF κB complexes:

$$\frac{d(i\kappa b)}{dt} = V_{I\kappa B}^{\max} p_{I\kappa B}^{on}(t) - k_4 i\kappa b \cdot nf \qquad (13)$$

where $V_{I\kappa B}^{\max}$ is the maximum rate of translation of *IκB*, and $p_{I\kappa B}^{on}(t)$ is the probability that the gene *IκB* is activated at time *t* (Table 1).

The rate of variation of the amount of the enzyme Cox2 in the system depends on the rate of translation of the *Cox2* gene, and its rate of inhibition by different mechanisms:

$$\frac{dcox2}{dt} = V_{Cox2}^{\max} p_{Cox2}^{on}(t) - k_{10} cox2 \qquad (14)$$

where *cox2* is the amount of the enzyme in the system, $V_{Cox2}^{\max}$ is the maximum rate of variation, $p_{Cox2}^{on}(t)$ is the probability that the gene *Cox2* is activated at time *t*, k_8, k_9 and k_{10} are rate constants (Table 1).

The rate of variation of the amount of PGE2 in the system depends on the amount of Cox2, on the amount of IL-6, and on its rate of degradation:

$$\frac{dpge2}{dt} = k_{17} cox2 - k11 pge2 \cdot i\kappa bnf - k_{12} pge2 \qquad (15)$$

where k_{11}, k_{12} and k_{17} are rate constants (Table 1).

3 Results

In this section we discuss only the results that are relevant to understand the role of Nsp5 in the process of acute lung inflammation. Results related to the mathematical aspects of the model are reported in SM 2.

We solved the model using the Euler predictor-corrector method with time step of 0.05 s and 720,000 integration steps to simulate a period of 10 hrs post infection, which is the estimated time

Preprints (www.preprints.org) | NOT PEER-REVIEWED | Posted: 30 December 2020 doi:10.20944/preprints202012.0749.v1

for the first bursting of new virions into the extracellular medium (Bar-On et al., 2020). We used the parameter values shown in Table 1 to generate an *arbitrary reference state* (ARS) of the system for the initial conditions $i\kappa bnf = 5$ (nM), and 0 at time $t = 0$ for the rest of the variables. In this case, the input $\alpha(t) = 10$ nM s^{-1} and $nsp5 = 0$ for $t \in [0, \infty)$. In this ARS, the translation velocities of all genes are set to 2 nM s^{-1} (Hauser et al., 2019). Figure 4A shows that the output of the model is the transitory activation of NF κB, Cox2 and PGE2, in contrast with a sustained high activation of IL-6. In order to clarify the source of the steady activation of IL-6, we solved the model with the same initial conditions and $\alpha(t) = 0$. In this case, the system does not *turn on* during all the time of simulation (data not shown), indicating that the signal from monocytes and other cells is a *necessary condition* to start the IL-6 sustained production in lung cells (Figure 4A). Figure 4B shows that when $nsp5 \neq 0$, $\alpha(t) = 0$ and equal gene translation rates, the response of the system is a high sustained level of activation of NF κB, Cox2, and PGE2 with respect to the ARS. In this case, the concentration of IL-6 in the cell was only slightly affected by the virus. Figures from 4A to 4D show only the first five minutes of simulation for which the circuit of Figure 2 reaches its steady state.

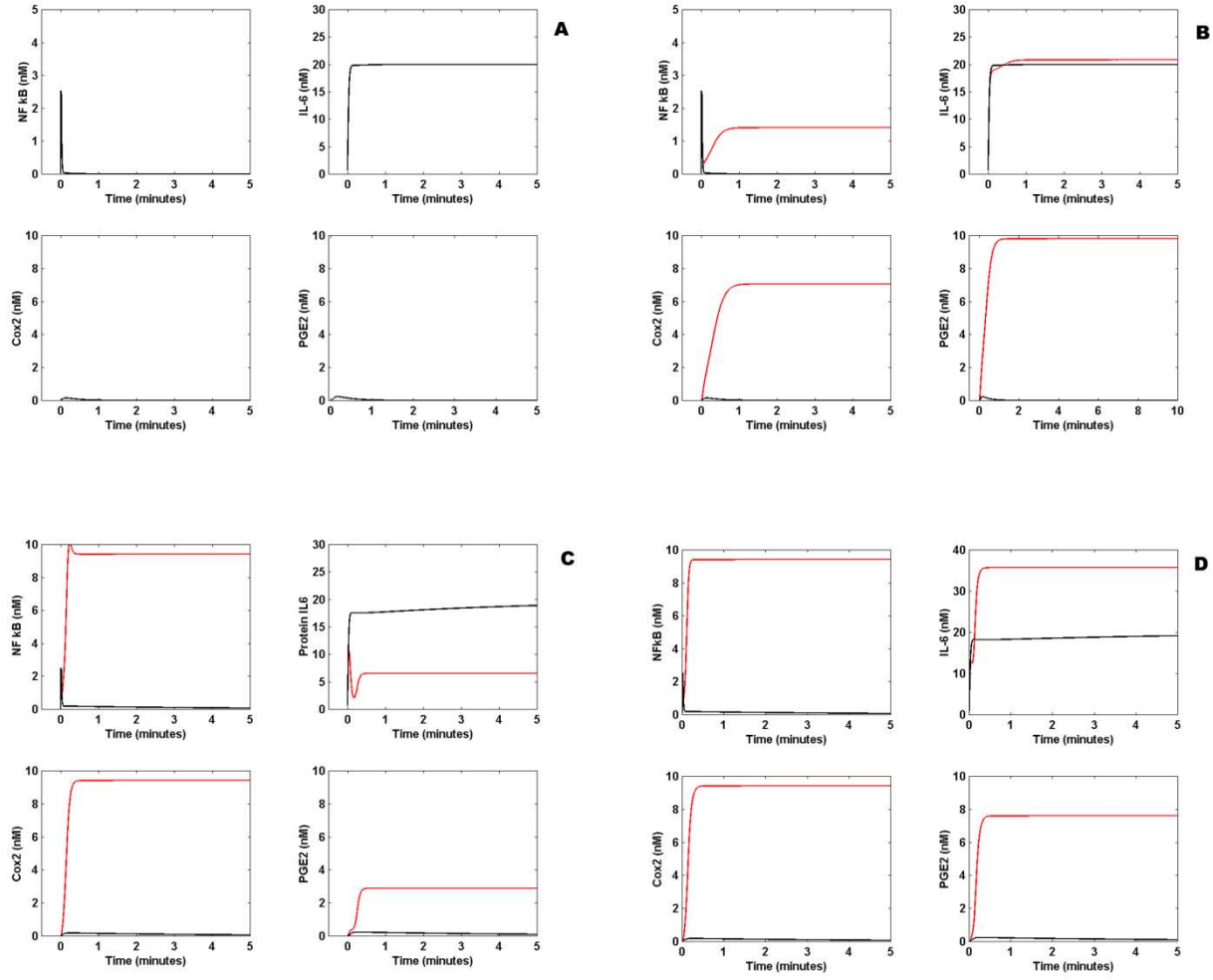

Figure 4.- Effect of Nsp5 on IL-6 production. A) Arbitrary reference state (ARS) of the circuit of Figure 2. In absence of the viral protein Nsp5, the response to an external input $a(t) = 10$ nM s^{-1} is a transitory activation of NF κB, Cox2, and PGE2. In this case, IL-6 shows a steady high concentration. In this case, all the gene translation rates are set to 2 nM $^{s-1}$. B) In presence of Nsp5 the circuit shows steady higher

Preprints (www.preprints.org) | NOT PEER-REVIEWED | Posted: 30 December 2020 doi:10.20944/preprints202012.0749.v1

concentrations of NF κB, Cox2, and PGE2 (red line) with respect to ARS (black line). IL-6 steady concentration (black line) is unaffected by the presence of the viral protein (red line). In this panel, $a(t)$ = 10 nM s^{-1} and all the gene translation rates are set to 2 nM $^{s-1}$. C) When NF κB and IκB translation rates are $V_{nf}^{\max} = 10$ nM s^{-1} and $V_{I\kappa B}^{\max} = 15$ nM s^{-1}, respectively, and Cox2 and IL-6 translation rates are 2 nM s^{-1} the circuit shows a weak sustained activation of NF κB, Cox2, and PGE2 (black line) in response to the external input $\alpha(t)$ = 10 nM s^{-1} and in absence of Nsp5. In this case, IL-6 steady concentration does not change (black line). In presence of Nsp5 the circuit shows steady higher concentrations of NF κB, Cox2, and PGE2 (red line), although the concentration of IL-6 is lower than is absence of the virus. D) In the over stimulated immune state (OSIS), the presence of Nsp5 produces an enhanced production of NF κB, Cox 2, PGE2 and IL-5 (red lines). This particular state is obtained when $\alpha(t)$ = 10 nM s^{-1}, $V_{nf}^{\max} = 10$ nM s^{-1}, $V_{I\kappa B}^{\max} = 15$ nM s^{-1}, $V_{Cox2}^{\max} = 2$ nM s^{-1}, and $V_{IL6}^{\max} = 20$ nM s^{-1}.

Translation rates of the set of genes of the model rarely have the same value, even when they activation is promoted by the same transcription factor (NF κB in this case). As shown in Table 1, the results of Figures 4A and 4B are obtained when the rates of translation are the same for all genes. However, in real cells this is not the case, and *Cox2*, *Il-6*, *NF κB* and *IκB* are translated at different rates. In *Homo sapiens* the estimated average rate of translation ($V^{\max}$) of a gene is about 10^4 proteins per hour (Hausser et al., 2019), which is equivalent to ~ 1 nM s^{-1} in a cell of 10 μm of diameter. However, this average value can be increased according to the state of activity of the cell. In the present work, we arbitrary chose the value of $V^{\max} = 2$ nM$\cdot s^{-1}$ for all genes in the ARF (Table 1). However, we made parameter variation to know how different values of this set of parameters affect the qualitative behavior of the model (SM 2). Figure 4C shows that when in the system $V_{nf}^{\max} = 10$ nM$\cdot s^{-1}$, $V_{I\kappa B}^{\max} = 15$ nM$\cdot s^{-1}$, $V_{Cox2}^{\max} = 2$ nM$\cdot s^{-1}$, and $V_{IL6}^{\max} = 2$ nM$\cdot s^{-1}$, $\alpha(t)$ = 10 nM s^{-1} and *nsp5* = 0, the circuit tends to a steady state in which NF κB, Cox2, and PGE2 exhibit a constant low concentration during the time of simulation, while IL-6 steady concentration is unaffected with respect to the value shown in Figure 4A. When *nsp5* ≠ 0, the steady concentration of NF κB, and Cox2, are increased ~ 10 fold with respect to their maximum concentration in the ARS, while PGE2 concentration is increased ~ 4 fold; Nsp5 produces a ~ 4 fold decrease in IL-6 steady concentration with respect to the reference concentration shown in Figure 4A.

Figure 4D shows that when $\alpha(t)$ = 10 nM s^{-1}, *nsp5* = 0, $V_{nf}^{\max} = 10$ nM$\cdot s^{-1}$, $V_{I\kappa B}^{\max} = 15$ nM$\cdot s^{-1}$, $V_{Cox2}^{\max} = 2$ nM$\cdot s^{-1}$, and $V_{IL6}^{\max} = 20$ nM$\cdot s^{-1}$ the circuit tends to a steady state in which NF κB, Cox2 and PGE2 exhibit a constant low concentration during the time of simulation, while IL-6 is unaffected with respect to its steady concentration in Figure 4A. However, when *nsp5* ≠ 0 the dynamical behavior of the circuit changes because NF κB and Cox2 show the same steady concentration that in Figure 4C, but PGE2 has a higher steady concentration. In this case, IL-6 shows an increase of ~ 2 fold with respect to the level shown in Figure 4C.

All these results suggest some important dynamical properties of the circuit of Figure 2: a) Nsp5 increases the concentration of NF κB, Cox2 and PGE2 in the circuit, when $\alpha(t)$ = 10 nM s^{-1}, independently of the value of $V_{IL6}^{\max}$; b) an increment in the values of $V_{nf}^{\max}$ and $V_{I\kappa B}^{\max}$, produce enhanced concentrations of NF κB, Cox2 and PGE2 in the circuit in presence of Nsp5, when $\alpha(t)$ = 10 nM s^{-1}, independently of the value of $V_{IL6}^{\max}$; c) the circuit has high sensitivity to the value of

Preprints (www.preprints.org) | NOT PEER-REVIEWED | Posted: 30 December 2020 doi:10.20944/preprints202012.0749.v1

V_{IL6}^{max}: a high value of this parameter produces an over production of NF κB, Cox2, PGE2, and IL-6 in the circuit in presence of Nsp5 and $\alpha(t)$ = 10 nM s^{-1}, with respect to the ARS (Figures 4A and 4D). We named *over stimulated immune state* (OSIS) to the state of the system shown in Figure 4D, for which: V_{nf}^{max} = 10 nM s^{-1}, $V_{I\kappa B}^{max}$ = 15 nM s^{-1}, V_{Cox2}^{max} = 2 nM s^{-1} , V_{IL6}^{max} = 20 nM s^{-1} and $nsp5 \neq 0$.

Figure 5 shows the response of the circuit to a step function defined as:

$$\alpha(t) = \begin{cases} 10 & 0 \le t < 10 \\ 0 & t > 10 \end{cases} \qquad (16)$$

which simulates an external signal of IL-6 initially generated at a rate of 10 nM s^{-1} during 10 minutes, and switched *off* after 10 minutes. Figure 5A is the response of the system in ARS to the step signal, in absence and presence of Nsp5. In absence of Nsp5, the circuit exhibits a low concentration of NF κB, Cox2 and PGE2, and a high concentration of IL-6, all which are zero when the external signal is switched *off*. In presence of Nsp5 the ARS is perturbed by $\alpha(t)$, and reaches a new steady state with high concentrations of NF κB, Cox2, and PGE2 that remain even when the external signal is switched *off*. Furthermore, the high IL-6 concentration reached when the circuit is turned *on* falls to a lower concentration different from zero when $\alpha(t)$ = 0.

Figure 5B is the response of the circuit in OSIS to the step function. In absence of Nsp5, the circuit exhibits a low concentration of NF κB, Cox2 and PGE2, and a high concentration of IL-6, all which are zero when the external signal is switched *off*. However, in presence of Nsp5 the OSIS is perturbed by $\alpha(t)$, and reaches a new steady state with high concentrations of NF κB, Cox2, and PGE2 that remain even when the external signal is switched *off*. Furthermore, the higher IL-6 concentration reached when the circuit is turned *on* only falls ~ 50% of its maximum concentration when $\alpha(t)$ = 0. These results suggest that the OSIS becomes *autonomous* of the external signal generated by monocytes and other immune cells in response to Nsp5, i.e., *the OSIS becomes a persistent state that never shut down by itself, or by removing external signaling, in presence of SARS-CoV-2*.

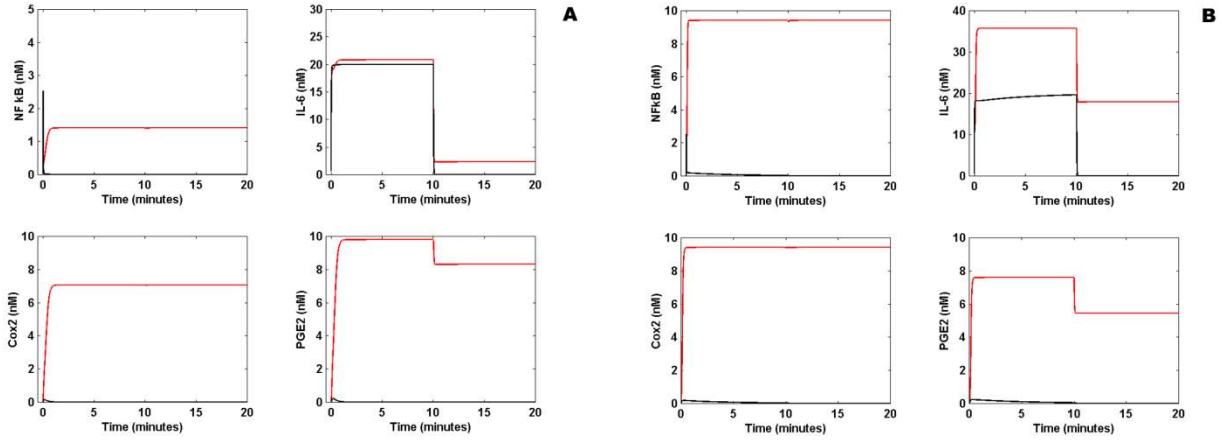

Figure 5.- Response of the circuit to a step function. A) When the external signal $\alpha(t)$ is the step function of Eq. (16) of main text and is applied to the ARS in absence of Nsp5 (black line) the level of cytokine IL-6 initially increases to a maximum value of 20 nM, and becomes zero when the external signal is switched *off*. There is not any effect on NF κB, Cox2 and PGE2 concentrations in the circuit. However, in presence of Nsp5 (red line) the levels of NF κB, Cox2, PGE2 and IL-6 are increased in response to $\alpha(t)$ and never

Preprints (www.preprints.org) | NOT PEER-REVIEWED | Posted: 30 December 2020 doi:10.20944/preprints202012.0749.v1

become zero when the external signal is switched *off*. B) When the step function of Eq. (16) is applied to the circuit in absence of Nsp5 (black line) with $V_{nf}^{\max} = 10$ nM s^{-1}, $V_{I\kappa B}^{\max} = 15$ nM s^{-1}, $V_{Cox2}^{\max} = 2$ nM s^{-1}, and $V_{IL6}^{\max} = 20$ nM s^{-1}, there is a low increase in NF κB, Cox2 and PGE2 concentrations that becomes zero when the external signal is switched *off*. IL-6 initially increases to a maximum value of 20 nM, and becomes zero when the external signal is also zero. In contrast, when the circuit is in OSIS in presence of Nsp5 (red line) the concentrations of NF κB, Cox2, PGE2 and IL-6 are increased in response to $\alpha(t)$ and remain at a high value even the external signal is switched *off*.

In order to reduce the effect of Nsp5 on the circuit of Figure 2, we test the effect of Nimesulide on NF κB production. Nimesulide, a Cox2 inhibitor, acts inhibiting the synthesis of Cox2 and lipooxigenase enzyme and products (Suleyman et al., 2008). We modified Eq. (14) to introduce an inhibition term that decreases the rate of production of Cox2 in presence of Nimesulide:

$$\frac{dcox2}{dt} = \frac{V_{Cox2}^{\max} p_{Cox2}^{on}(t)}{nim+1} - k_{10} cox2 \qquad (17)$$

where *nim* is the amount of Nimesulide at time *t*, whose rate of variation of its concentration in the cell is:

$$\frac{d(nim)}{dt} = r_2 - k_{19} nim \qquad (18)$$

where $r_2 = 40$ nM s^{-1} and $k_{19} = 3$ s^{-1}. Solution of the modified model (Eq. 17) is presented in Figure 6. In Figure 6A, Nimesulide is applied to the circuit in presence of Nsp5, and with all gene translational rates set to 2 nM s^{-1}. In this case, Nimesulide has no effect on NF κB, a slightly effect on IL-6, and a significant decrease in Cox2 and PGE2 concentrations to values near to zero in presence of 14 nM of the drug. The same effect is observed when the circuit is in OSIS (Figure 6B). Thus, Nimesulide has incomplete anti-inflammatory effects, and does not impact the concentration of IL-6 in the circuit in presence of Nsp5, even increasing its concentration.

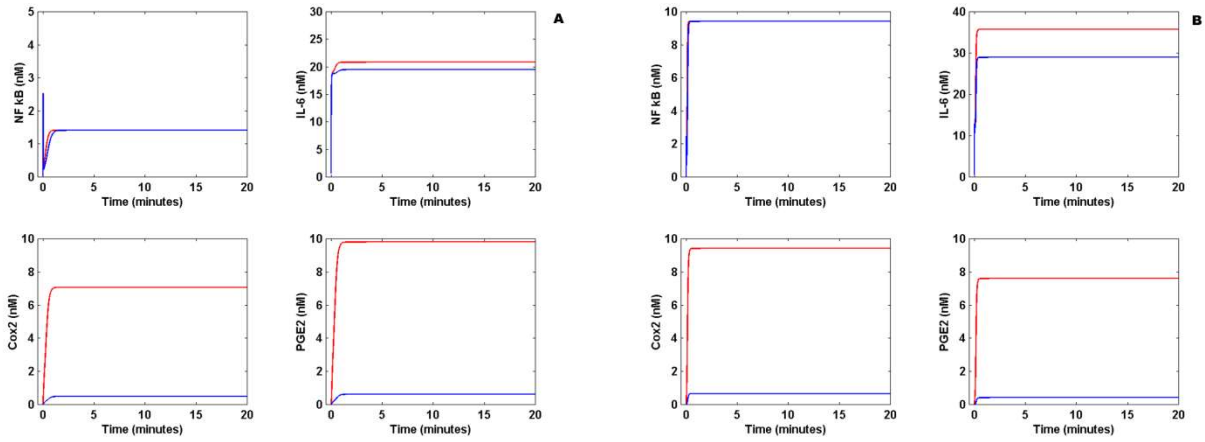

Figure 6.- Effect of Nimesulide on lung cell inflammation. A) Effect of 14 nM of Nimesulide on the levels of NF κB, Cox2, PGE2 and IL-6 when $\alpha(t) = 10$ nM s^{-1}, and all gene translation rates are 2 nM s^{-}

Preprints (www.preprints.org) | NOT PEER-REVIEWED | Posted: 30 December 2020 doi:10.20944/preprints202012.0749.v1

[1] in presence of Nsp5 (red line). Nimesulide decreases the concentration of Cox2 and PGE2, but has not effect on NF κB and IL-6 (blue line). B) Effect of 14 nM of Nimesulide on the OSIS (red line). Nimesulide significantly decreases the concentration of Cox2 and PGE2, but has not effect on NF κB, The drug has a weak effect on IL-6 concentration (blue line).

Another anti-inflammatory drug is Dexamethasone (DX), a potent synthetic glucocorticoid that inhibits NF κB transcription. In order to test the effect of DX on the inflammatory process in the circuit of Figure 2, we modified Eq. (8) to introduce an inhibition term that decreases the probability of activation of *NF κB*:

$$\frac{dp_{NF\kappa B}^{on}(t)}{dt} = k_{15}\left(\frac{nf*}{(hd*+1)(DX+1)}\right)\left(1-p_{NF\kappa B}^{on}(t)\right)-k_{-15}p_{NF\kappa B}^{on}(t) \qquad (19)$$

where *DX* is the amount of DX at time *t*, whose rate of variation of its concentration in the cell is:

$$\frac{d(DX)}{dt} = r_3 - k_{20}DX \qquad (20)$$

where r_3 = 30 nM s^{-1} and k_{20} = 3 s^{-1}.

Figure 7 shows the effect of DX on the circuit. Figure 7A shows that when DX is applied to the circuit in presence of Nsp5, and when all genes have the same translational rate of 2 nM s^{-1}, the drug eliminates NF κB, Cox2 and PGE2 from the circuit, but has a null effect on the concentration of IL-6. However, when the circuit is in OSIS (Figure 7B), DX has little effect on the immune response in presence of Nsp5. Figure 7C shows that when all translation rates are the same (2 nM s^{-1}), DX can shut down the immune response in presence of the virus, when the circuit input $\alpha(t)$ is the function of Eq. (16). However, DX cannot shut down the effects of Nsp5 when the circuit is in OSIS, having a little anti-inflammatory effect (Figure 7D). In this form, these results suggest that DX *is an effective anti-inflammatory drug during mild inflammatory state, but not during acute lung inflammation due to SARS-CoV-2*. This dynamical behavior of the circuit of Figure 2 is unaffected by higher doses of DX. When DX and Nimesulide are applied together (with 35 nM of DX and 40 nM of Nimesulide) to the circuit in OSIS, in which $\alpha(t)$ is the function of Eq. (16), there is also a little anti-inflammatory effect (Figure 8A).

However, the molecular docking of Nsp5 with a hypothetical drug like Saquinavir (Xu et al., 2020), completely eliminates inflammation. This point can be test modifying the term of Nsp5 production in Eq. (11) with an inhibitory term:

$$\frac{d(nsp5)}{dt} = \frac{\phi}{drug+1} - k_{18}nsp5 \qquad (20)$$

where *drug* is the amount of the hypothetical drug that can remove Nsp5 from the circuit, whose concentration at time *t* is given by:

$$\frac{d(drug)}{dt} = r_4 - k_{21}drug \qquad (21)$$

Preprints (www.preprints.org) | NOT PEER-REVIEWED | Posted: 30 December 2020 doi:10.20944/preprints202012.0749.v1

with $r_4 = 30$ nM s^{-1} and $k_{21} = 3$ s^{-1}.

Figure 8B shows that when the hypothetical drug is applied to the circuit in OSIS, with $\alpha(t)$ given by Eq. (16), the inflammation process is completely shut down, suggesting *that Nsp5 is effectively the cause of the acute lung inflammation during SARS-CoV-2 infection*.

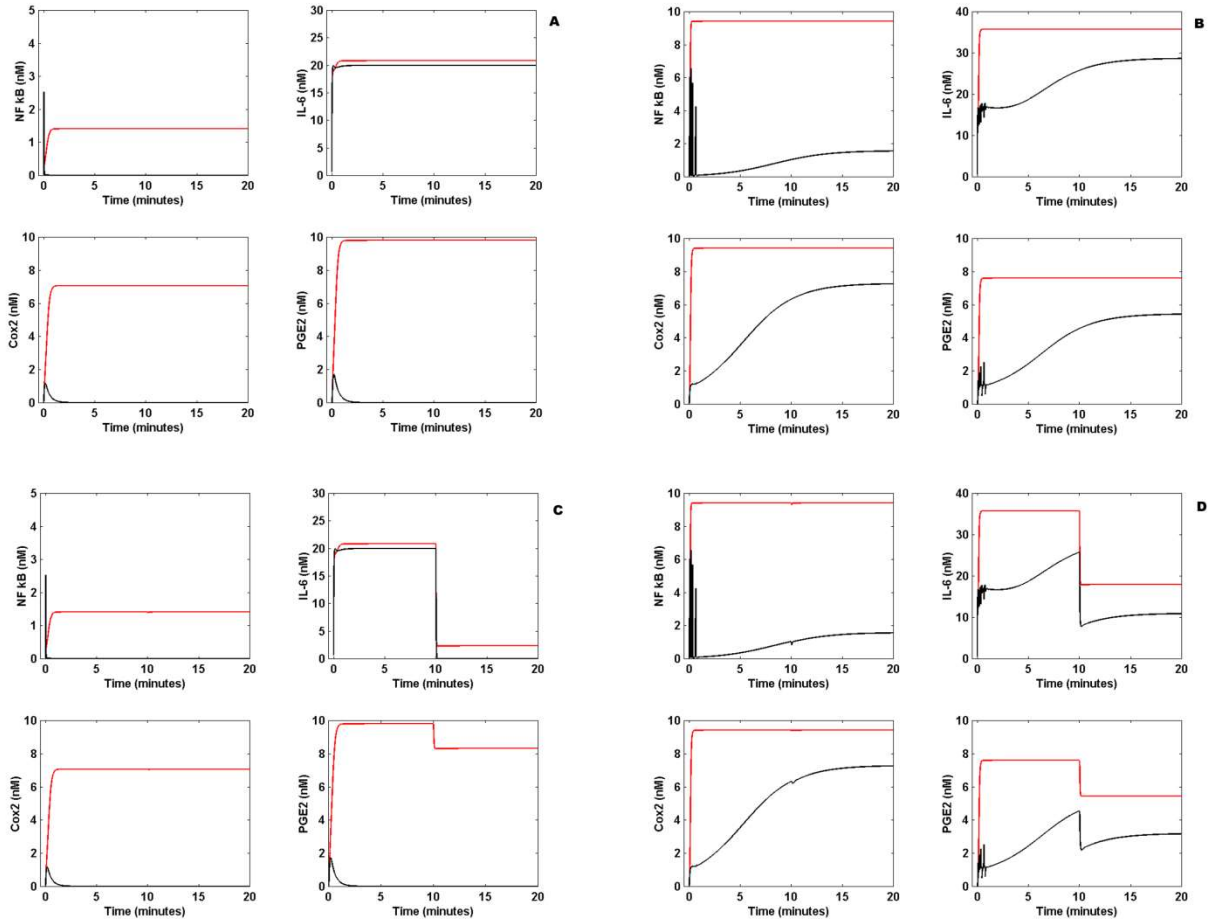

Figure 7.- Effect of Dexamethasone on lung cell inflammation. A) Effect of 14 nM of Dexamethasone (DX) on the levels of NF κB, Cox2, PGE2 and IL-6 when $a(t) = 10$ nM s^{-1}, and all gene translation rates are 2 nM s^{-1} in presence of Nsp5 (red line). DX effectively decreases the concentration of NF κB, Cox2 and PGE2 to cero, but has not effect on IL-6 (black line). B) Effect of 14 nM of DX on the OSIS (red line). DX has a weak effect on the concentration of NF κB, Cox2, PGE2, and IL-6 (red line). C) When the external signal $a(t)$ is the step function of Eq. (16) of main text and is applied to the circuit in presence of Nsp5 (red line), with all gene translation rates equal to 2 nM s^{-1}, 14 nM of DX decreases the concentration of NF κB, Cox2, PGE2 and IL-6 to zero (black line). D) When the external signal $a(t)$ is the step function of Eq. (16) of main text and 14 nM of DX are applied to the circuit in the OSIS, the drug has a practically null effect on the inflammation process.

Preprints (www.preprints.org) | NOT PEER-REVIEWED | Posted: 30 December 2020 doi:10.20944/preprints202012.0749.v1

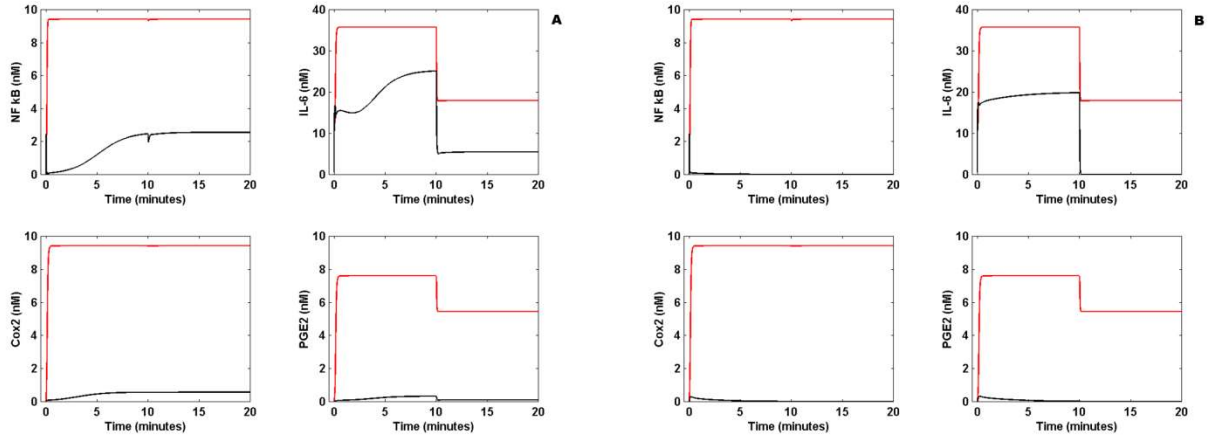

Figure 8.- Effect of the molecular docking of Nsp5 on lung inflammation. A) When DX and Nimesulide are applied together (with 35 nM of DX and 40 nM of Nimesulide) to the circuit in OSIS (red line), in which $\alpha(t)$ is the function of Eq. (16), there is also a little anti-inflammatory effect. B) The molecular docking of Nsp5 completely shuts down the inflammation process when the circuit is in OSIS, with $\alpha(t)$ given by Eq. (16), suggesting that Nsp5 is effectively the cause of the acute lung inflammation during

4 Discussion

The complexity of the immune response to infection resides on the set of different kinds of cells that secrete a great number of diverse molecules that produce different specific responses. All these elements are integrated into the network responsible of the inflammation process whose dynamical properties depend on its structure, i.e., the number of nodes, links, and the distribution of links between the nodes (Eftimie et al., 2016; Morel et al., 2006). The structure of this network is not random due to the specific nature of its nodes and links, so that if the network has a hierarchical structure its hubs determine the overall network dynamics and the structure of its phase space (Eftimie et al., 2016; Díaz. 2020b; Cessac, 2009). In high dimensional phase spaces, steady points of diverse kinds can coexist with isolated closed curves (limit cycles), strange attractors of fractal structure, and other limit sets giving rise to a variety of biological dynamical behaviors like molecular switches, periodic and quasi-periodic oscillations, and bursting (among others). Two central problems in the analysis of this kind of dynamical systems are: a) the structure of the phase space is strongly dependent of the value of the set of parameters of the dynamical system, and b) the nonlinearity of biological systems (see SM 2) (Nayak et al, 2018).

In most of the ODEs-based biological models so far studied there is a gap in the knowledge of the real value of the parameters, which leads to an uncertainty in the extent in which the model explains the real process under study. In this case, the validation of the model lays on experimental data from experiments specially designed to test the predictions of the model. However, beside some particular cases (Hodgkin and Huxley, 1952), as this kind of modeling is qualitative its predictions are also of qualitative nature, and their agreement with quantitative experimental data is difficult to test (Eftimie et al., 2016). This problem increases with the dimensionality of the model. Thus, is necessary to choose some particular properties of the network under study (inflammation network in this case) that reflect the important dynamical features of it, and that can also aid to reduce the number of parameters of the model to the minimum possible.

Preprints (www.preprints.org) | NOT PEER-REVIEWED | Posted: 30 December 2020 doi:10.20944/preprints202012.0749.v1

In this sense, we limit the scope of this work to the study of the inflammation process of epithelial lung cells during SARS-CoV-2 infection. The epithelial lung cells form a sub-network that have two highly connected nodes: the internal signal integrator NF κB, and the external signal integrator IL-6 Receptor (IL6R) (Magro, 2020), which is activated by external IL-6 (Figures 2 and 3). Both integrators trigger the activation of two important intermediate processes: Cox2 and PGE2 synthesis. Thus, we propose, as a first approximation, that the dynamical behavior of this these four nodes of the circuit of Figure 2 reflect with certain accuracy the dynamical properties of the complex inflammation sub-network of lung cells. Thus, the dynamics of IL-6, NF κB, Cox2 and PGE2 nodes is described by a model that consist of 12 nonlinear coupled ordinary differential equations (Table 1), which we assume represents the central aspects of the dynamics of the lung cells inflammation process based on the temporal dynamics of the three coupled feedback loops of Figure 3. Then, we use this low-dimensionality model to explore the effect of Nsp5 in the qualitative dynamics of the inflammation circuit of Figure 2 (Diaz, 2020b).

SARS-CoV-2 main protease Nsp5 has a role as an epigenetic regulator of host DNA expression in lung cells; its physical association with HADC2 (Gordon et al., 2020) avoids the movement of the deacetylase from the cytoplasm to the nucleus, increasing the probability of the binding of NF κB to the promoter site of its target genes (Eqs. 5-8) (El Baba & Herbein, 2020). NF κB is a central integrator of the signals that initiate the inflammation process (Figure 1), which include IL-6 secreted by monocytes, leucocytes, macrophages, among other cells, together with signals from TLR4 and TLR7 that suppress the IκB-NF κB complex in a MyD88 independent manner (Vidya et al., 2017) . NF κB enhanced transcriptional activity includes the transcription of *IL-6*, *Cox2*, *IκB* and *NF κB* itself that are key genes in the process of inflammation (Figure 3).

Results obtained from our model suggest that Nsp5 can effectively transform a weak inflammation response into a persistent sustained one that has a relative high concentration of the cytokine IL-6 (Figure 4B). In the example of Figure 4B, all genes have the same translation rate, a condition that have low probably of occurrence in the real human immune system in which every gene is subject to different processes of post transcriptional regulation (Hausser et al., 2019). When this restriction is removed, and IL-6 has a high translation rate, Nsp5 boosts the concentration of the four main proteins of the circuit with respect to their respective values in ARS, and the inflammation response becomes strongly persistent with a high IL-6 concentration. Furthermore, in this state that we named OSIS, the dynamics of the circuit of Figure 2 becomes independent of any kind of external signal and never turns *off*, leading to the deregulation of the production of the cytokine IL-6 (Figure 5B). In this form, Nsp5 changes the qualitative dynamical behavior of the system, in which the trajectories that initially span around the ARS stable node now span around the OSIS stable node (see SM 2) (Díaz, 2020b).

An important biological consequence of this change in the qualitative dynamics of the circuit is that ACE2 receptor synthesis also becomes persistent and autonomous of any external signal to the lung cells (Figure 2). Furthermore, neither Nimesulide nor Dexamethasone or both can eliminate the OSIS suggesting that this dynamical behavior could be the form in which the virus assures the persistence of its reproductive cycle without any perturbation from the natural defenses of the body. This can be also a possible clue about the reason of the substitution of N protein used in SARS-CoV for the use of the main protease Nsp5 in SARS-CoV-2 as the switch for the inflammation process, which is necessary for ACE2 sustained production, taking into consideration that SARS-CoV N protein targets Cox2 while SARS-CoV-2 Nsp5 protein targets the master integrator NF κB. If this hypothesis is true, *this is the probable reason of the increased dangerousness of SARS-CoV-2 with respect to SARS-CoV*.

Preprints (www.preprints.org) | NOT PEER-REVIEWED | Posted: 30 December 2020 doi:10.20944/preprints202012.0749.v1

It is of interest that the persistence of the OSIS is supported by a high translational rate of *IL-6*, which in the model must have a value of $V_{IL6}^{\max} \geq 7$ nM s^{-1}. This result pictures a probable hypothetical scenario where the external signal $\alpha(t)$ triggers the initial inflammation response with a low translational rate of IL-6 that can be shut down with DX. As viral infection continues, IL-6, NF κB, and IκB increase their rate of translation ($V_{Cox2}^{\max}$ value has a little weight in this process) and the dynamical behavior of the circuit of Figure 2 becomes independent of the value of $\alpha(t)$, and *self-sustained*, i.e., the control of the production of the cytokine IL-6 is translated from the external immune cells to the lung cells, and cannot be stopped even with high doses of DX. In this form, in the model, $V_{IL6}^{\max}$ *is a bifurcation parameter* that changes the qualitative dynamical behavior of the circuit of Figure 2 when $V_{nf}^{\max} = 10$ nM s^{-1} and $V_{I\kappa B}^{\max} = 15$ nM s^{-1} have constant values (see SM 2).

In this extreme situation (OSIS), the unique treatment possible suggested by our model is an inhibitor of Nsp5 like *Saquinavir* (Xun et al., 2020). In this case, the OSIS is completely shut down, which indirectly implies the down production of ACE2. Saquinavir is an anti-retroviral drug used against the main protease of HIV-1 (Bensussen et al., 2018; Xun et al., 2020), with some undesirable effects like diarrhea, abdominal pain, and nausea. This could be a plausible treatment against the effects of SARS-CoV-2 in acute lung inflammation, and as a complement to the new vaccine against this coronavirus.

In a previous work (Díaz, 2020a) the role of the viral protein Orf8 as a hub of the SARS-CoV-2 infection was suggested. This highly connected protein has as main targets those processes related to the vesicular trafficking required for the ensemble of new virions (Figure 1) (Gordon et al., 2020). Thus, the inhibition of the effects of Orf8 in the host cells could block the reproduction cycle of the virus but not the inflammation process because Nsp5 is not directly linked to Orf8 (Gordon et al., 2020). Rapamycin has been suggested as a drug against the effects of Orf8 but produces severe immunosuppressant effects, which, according to the results of our model, will not be of care in cases of severe lung inflammation because Nsp5 uncouple the circuit of Figure 2 from the process of viral replication (Figure 1 and Figure 5B). In this case, a treatment with Rapamycin and Saquinavir can be an alternative for patients with severe lung inflammation. This suggestion needs experimental verification and clinical evaluation.

5 Conclusions

In this work we propose a model of the process of inflammation of lung cells in response to SARS-CoV-2 infection from which a plausible scenario for the dynamics of this process arises. In this scenario the main protease Nsp5 effectively enhances the inflammatory process, increasing the levels of NF κB, IL-6, Cox2, and PGE2 with respect to the reference state. When the translation rates of NF κB and IκB are increased to a high constant value, and the translation rate of IL-6 is increased above the threshold value of 7 nM s^{-1} the circuit enters in a persistent over stimulated immune state (OSIS) with high levels of the cytokine IL-6. The OSIS never shuts down by itself, and becomes autonomous of the signals from other immune cells like macrophages and lymphocytes. DX or Nimesulide have little effect on the OSIS, and the only form of suppress it is by inhibition of protein Nsp5 with drugs like Saquinavir.

In this form, the model suggests, in accordance to our hypothesis, that Nsp5 is effectively the cause of severe acute lung inflammation during SARS-CoV-2 infection. The persistent production of IL-6 by lung cells during infection can be one of the causes of the cytokine storm observed in critical

patients with COVID19. From an evolutive point of view, the use of Nsp5 as the switch to start inflammation, and the consequent overproduction of the ACE2 receptor, is the probable reason of the increased pathogenicity of SARS-CoV-2 with respect to SARS-CoV.

The present work is part of the project "Dynamics of the SARS-CoV-2 network" and is based on the experimental data available at the moment.

6 Conflict of Interest

The authors declare that the research was conducted in the absence of any commercial or financial relationships that could be construed as a potential conflict of interest.

7 Author Contributions

Antonio Bensussen made the stability and sensitivity analysis of the model. Elena R. Álvarez-Buylla and José Díaz equally contributed to this work.

8 Funding

This work was supported by CONACYT, and by the PRODEP funding program of the Universidad Autónoma del Estado de Morelos. Antonio Bensussen was supported CONACYT Postdoctoral grant number .

9 Acknowledgments

José Díaz thanks Erika Juarez Luna for logistical support.

10 References

Aghai, Z, H., Kumar, S., Farhath, S. et al. (2006). Dexamethasone suppresses expression of Nuclear Factor-kappaB in the cells of tracheobronchial lavage fluid in premature neonates with respiratory distress. *Pediatr Res* 59:811-815. doi: 10.1203/01.pdr.0000219120.92049.b3

Alexanian, A., and Sorokin, A. (2017). Cyclooxygenase 2: protein-protein interactions and posttranslational modifications. *Physiol Genomics* 49: 667–681. doi: 10.1152/physiolgenomics.00086.2017: 10.1152/physiolgenomics.00086.2017

Bai, D., Ueno, L., and Vogt, P.K. (2009). Akt-mediated regulation of NFκB and the essentialness of NFκB for the oncogenicity of PI3K and Akt. *Int J Cancer*. 125:2863–2870. doi:10.1002/ijc.24748

Bar-On, Y., Flamholz, A., Phillips, R., and Milo, R. (2020). SARS-CoV-2 (COVID-19) by the numbers. *eLife* 9:e57309. doi: https://doi.org/10.7554/eLife.57309

Bartlam, M., Yang, H., and Rao, Z. (2005). Structural insights into SARS coronavirus protein. *Curr Opin Struct Biol* 15: 664-6672, dol: 10.1016/j.sbi.2005.10.004

Bensussen, A., Torres-Sosa, C., Gonzalez, R.A., and Díaz, J. (2018). Dynamics of the Gene Regulatory Network of HIV-1 and the Role of Viral Non-coding RNAs on Latency Reversion *Frontiers in Physiology* 9:1364. doi: 10.3389/fphys.2018.01364

Breitling, R. (2010). What is systems biology? *Frontiers in Physiology 1: 9.* doi: 10.3389/fphys.2010.00009

Bouffi, C., Bony, C., Courties, G., Jorgensen, C., Noël, D. (2010). IL-6-Dependent PGE2 Secretion by Mesenchymal Stem Cells Inhibits Local Inflammation in Experimental Arthritis. *PLoS ONE* 5(12): e14247. doi:10.1371/journal.pone.0014247

Cessac, B. (2009). A view of Neural Networks as dynamical systems. *arXiv*: 0901.2203v2 [nlin.AO]. doi: 10.1142/S0218127410026721

Cho, J., Han, I., Lee, H., R., and Lee, H. (2014). Prostaglandin E2 Induces IL-6 and IL-8 Production by the EP Receptors/Akt/NF-κB Pathways in Nasal Polyp-Derived Fibroblasts. Allergy Asthma. *Immunol Res*. 6: 449–457. doi: 10.4168/aair.2014.6.5.449

Cohen, R., Erez, K., ben-Avraham, D., and Havlin, S. (2000). Resilience of the Internet to random breakdowns. *Phys. Rev. Lett*. 85: 4626. doi: https://doi.org/10.1103/PhysRevLett.85.4626

Danos, V., Feret, J., Fontana, W., Harmer, R., and Krivine, J. (2007). Rule-based modelling of cellular signalling. In: CONCUR 2007—concurrency theory. Springer, Berlin, pp 17–41. doi: 10.1007/978-3-540-74407-8_3

Diaz, J. (2020a). SARS-CoV-2 Molecular Network Structure. *Front. Physiol*. 10 doi: https://doi.org/10.3389/fphys.2020.00870

Díaz, J. (2020b). SARS-Cov-2 Systems Biology. *Ann Syst Biol* 3(1): 029-032. doi: https://dx.doi.org/10.17352/asb.000009

Dongwan, K., Joo-Yeon, L., Jeong-Sun, Yang., Won, K.J., Narry K., V., and Hyeshik C. (2020). The architecture of SARS-CoV-2 transcriptome. *BioRxiv* preprint doi: https://doi.org/10.1101/2020.03.12.988865

El Baba, R., and Herbein, G. (2020). Management of epigenomic networks entailed in coronavirus infections and COVID-19. *Clin Epigenet* 12**:**118. doi: https://doi.org/10.1186/s13148-020-00912-7

Eftimie, R., Gillard, J.J., and Cantrell, D.A. (2016). Mathematical Models for Immunology: Current State of the Art and Future Research Directions. *Bull Math Biol* 78:2091–2134. doi: 10.1007/s11538-016-0214-9

Forster, P., Forster, L., Renfrew, C., and Forster, M. (2020). Phylogenetic network analysis of SARS-CoV-2 genomes. *PNAS* 117: 9241-9243. doi: www.pnas.org/cgi/doi/10.1073/pnas.2004999117

Gordon, D. E., Jang, G. M., Bouhaddou, M., et al. (2020). A SARS-CoV-2-Human Protein-Protein Interaction Map Reveals Drug Targets and Potential Drug-Repurposing. *BioRxiv* preprint. doi: https://doi.org/10.1101/2020.03.22.002386

Hausser, J., Mayo, A., Keren, L., and Alon, U. (2019). Central dogma rates and the trade-off between precision and economy in gene expression. *Nature Communications* 10: 68. doi: https://doi.org/10.1038/s41467-018-07391-8

Hamming, I., Timens, W., Bulthuis, M.L.C., Lely, A.T., Navis, G.J., and van Goor, H. (2004). Tissue distribution of ACE2 protein, the functional receptor for SARS coronavirus. A first step in understanding SARS pathogenesis. *J Pathol* 203: 631–637. doi: 10.1002/path.1570

Hodgkin, A.L., and Huxley, A.F. (1952). A quantitative description of membrane current and its application to conduction and excitation in nerve. *The Journal of Physiology*. **117** : 500–44. doi:10.1113/jphysiol.1952.sp004764

Jafarzadeha, A., Chauhanc, P., Sahac, B., Jafarzadehe, S., and Nematif, M. (2020). Contribution of monocytes and macrophages to the local tissue inflammation and cytokine storm in COVID-19: Lessons from SARS and MERS, and potential therapeutic interventions. *Life Sciences* 257: 118102. doi: https://doi.org/10.1016/j.lfs.2020.118102

Kumar, N., Mishra, B., Mehmood, A., Athar M., and Mukhtar, M.S. (2020). Integrative Network Biology Framework Elucidates Molecular Mechanisms of SARS-CoV-2 Pathogenesis. *BioRxiv* preprint doi: https://doi.org/10.1101/2020.04.09.033910

Letko, M., Marzi, A., and Munster, V. (2020). Functional assessment of cell entry and receptor usage for SARS-CoV-2 and other lineage B betacoronaviruses. *Nature Microbiology* 5:562–569. doi: https://doi.org/10.1038/s41564-020-0688-y

Lipniacki, T., Paszek, P., Brasier, A.R., et al. (2004). Mathematical model of NF-kB regulatory module. *Journal of Theoretical Biology* 228: 195–215. doi: https://doi.org/10.1016/j.jtbi.2004.01.001

Hennighausen, L., and Lee, H.K (2020). Activation of the SARS-CoV-2 receptor *Ace2* by cytokines through pan JAK-STAT enhancers. *BioRxiv* preprint. doi: https://doi.org/10.1101/2020.05.11.089045

Magro, G. (2020). SARS-CoV-2 and COVID-19: Is interleukin-6 (IL-6) the 'culprit lesion' of ARDS onset? What is there besides Tocilizumab? SGP130Fc. *Cytokine: X* 2: 100029. doi: https://doi.org/10.1016/j.cytox.2020.100029

Masters, P.S. (2006). The Molecular Biology of Coronaviruses. *Advances in Virus Research* 66, 193-292. doi: https://doi.org/10.1016/S0065-3527(06)66005-3

McBride, R., and Fielding, B.C. (2012). The Role of Severe Acute Respiratory Syndrome (SARS)-Coronavirus Accessory Proteins in Virus Pathogenesis. *Viruses* 4, 2902-2923; doi:10.3390/v4112902

Messina, M., Giombini, E., Agrati, C., Francesco Vairo, F., et al. (2020). COVID‐19: viral–host interactome analyzed by network based‐approach model to study pathogenesis of SARS‐CoV‐2 infection. *J Transl Med* 18:233. doi: https://doi.org/10.1186/s12967-020-02405-w

Morel, P.A., Ta'asan, S., Morel, B.F., et al. (2006). New Insights into Mathematical Modeling of the Immune System. *Immunologic Research* 36:157–165. doi: 10.1385/IR:36:1:157

Nakagawa, K., Lokugamage, K.G., and Makino S. (2016). Viral and Cellular mRNA Translation in Coronavirus-Infected Cells. *Advances in Virus Research*, Volume 96: 2016. Elsevier Inc. ISSN 0065-3527. doi: http://dx.doi.org/10.1016/bs.aivir.2016.08.001

Nayak, S.J., Bit, A., Dey, A., Mohapatra, B., and Pal, K. (2018). A Review on the Nonlinear Dynamical System Analysis of Electrocardiogram Signal. Journal of Healthcare Engineering Volume 2018, Article ID 6920420. doi: https://doi.org/10.1155/2018/6920420

Newton, R., Seybold, J., Kuitert, L.,M., E., Bergmanni, M., and Barnes, P., J. (1998). Repression of Cyclooxygenase-2 and Prostaglandin E2 Release by Dexamethasone Occurs by Transcriptional and Post-transcriptional Mechanisms Involving Loss of Polyadenylated mRNA. *The Journal of Biological Chemistry* 273: 32312–32321. doi: 10.1074/jbc.273.48.32312

Long, Q., Tang, X., Shi, Q., et al. (2020). Clinical and immunological assessment of asymptomatic SARS-CoV-2 infections. *Nature Medicine* 26: 1200–1204.

Rahman, I., and MacNee, W. (1998). Role of transcription factors in inflammatory lung diseases. *Thorax* **53**:601–612. doi: 10.1136/thx.53.7.601

Sevajol, M., Subbisi, L., Decroly, E., Canard, B., and Imbert, I. (2014). Insights into RNA synthesis, capping, and proofreading mechanisms of SARS-coronavirus. *Virus Research*. doi: http://dx.doi.org/10.1016/j.virusres.2014.10.008

Strogatz, S.H. (2015). Nonlinear dynamics and chaos with applications to Physics, Biology, Chemistry and Engineering. CRC Press, 2nd Edition. ISBN-13 : 978-0813349107

Suleyman, H., Cadirci, E., Albayrak, A., and Halici Z. (2008). Nimesulide is a Selective COX-2 Inhibitory, Atypical Non-Steroidal Anti-Inflammatory Drug. *Current Medicinal Chemistry 15:* 278-283. doi: 10.2174/092986708783497247

Vidya, M.K., Kumar, V.G., Sejian,V., et al. (2017). Toll-like receptors: Significance, ligands, signaling pathways, and functions in mammals. *International Reviews of immunology*. doi: https://doi.org/10.1080/08830185.2017.1380200

Wang, L., Walia, B., Evans, J., Gewirtz, A.T., Merlin, D., and Sitaramania, S.V. (2003). IL-6 Induces NF-kB Activation in the Intestinal Epithelia. *J Immunol* 171:3194-3201. doi: 10.4049/jimmunol.171.6.3194

Wu, A., Peng, Y., and Huang, B., (2020). Genome Composition and Divergence of the Novel Coronavirus (2019-nCoV) Originating in China. *Cell Host & Microbe*. https://doi.org/10.1016/j.chom.2020.02.001

Xun, C., Ke, Z., Liu, C., et al. (2020). Systemic In Silico Screening in Drug Discovery for Coronavirus Disease (COVID-19) with an Online Interactive Web Server. *J. Chem. Inf. Model*. doi: https://dx.doi.org/10.1021/acs.jcim.0c00821

Yan , X., Hao, Q., Mu, Y., et al. (2006). Nucleocapsid protein of SARS-CoV activates the expression of cyclooxygenase-2 by binding directly to regulatory elements for nuclear factor-kappa B and CCAAT/enhancer binding protein. *Int J Biochem Cell Biol* 38: 1417-1428. doi: 10.1016/j.biocel.2006.02.003.